Neurovascular Unit Model

Documentation for Code "OO-NVU Version 1.1.1"

A merged NVC model of a neuron, astrocyte, smooth muscle cell, endothelial cell, the mechanical vessel response, and the extracellular space.

by Emiel van Disseldorp Katharina Dormanns Sanne van der Lelij
Joerik de Ruijter Michelle Louise Goodman Eva Waldhauser
Moritz Burger Kon Zakkaroff Allanah Kenny Tim David*

September 19, 2016

*Corresponding author, Tim.david@canterbury.ac.nz

Contents

1 Release notes

1.1 Changes to the previous version

This version expands on version 1.1 with the addition of the extracellular space (ECS) compartment, shown schematically in Figure 1.

It is proposed here that the interaction between the ECS and PVS compartment is excluded from the model, for the following reasons: it is assumed that the PVS volume is orders of magnitude smaller than the ECS as the astrocytic endfoot closely surrounds the arteriole [13]. In addition, by including a diffusive flux between the PVS and ECS in the model, the astrocytic K^+ pathway - where K^+ released into the SC during neuronal stimulation travels from the SC through the astrocyte and into the PVS - is effectively short circuited via the ECS and the astrocyte is bypassed. As such it is more physiologically realistic to model the PVS and ECS as completely separate spaces with no diffusive flux between them.

Diffusion of K^+ between the ECS and SC compartments of a single NVU is implemented via a linear diffusion term:

$$J_{diff} = \frac{1}{\tau_s}\left(K_e - K_s\right), \tag{1}$$

where J_{diff} is added to or subtracted from the differential equation for the K^+ concentration in the SC (K_s) and the K^+ concentration in the ECS (K_e) respectively. τ_s is the characteristic time that is needed for K^+ to diffuse over some distance Δx:

$$\tau = \frac{(\Delta x)^2}{2D_K}, \;\; D_K = \frac{D_{free}}{\lambda_0^2}. \tag{2}$$

Here D_K is the effective diffusion coefficient of K^+, D_{free} is the diffusion coefficient of K^+ in a free medium, and λ_0^2 is a tortuosity factor which is necessary because diffusion is hindered by the narrow confines of the ECS [12].

For diffusion between the ECS and SC, $\tau_s = 2.8$ based on an average astrocyte length (across two astrocyte arms) of 100 μm. The ECS is directly connected to the SMC via a calcium activated K^+ channel and sodium potassium pump (with fluxes denoted by J_K and J_{NaK} respectively) given by:

$$J_K = G_K w_i (v_i - v_K) \tag{3}$$

$$J_{NaK} = F_{NaK}. \tag{4}$$

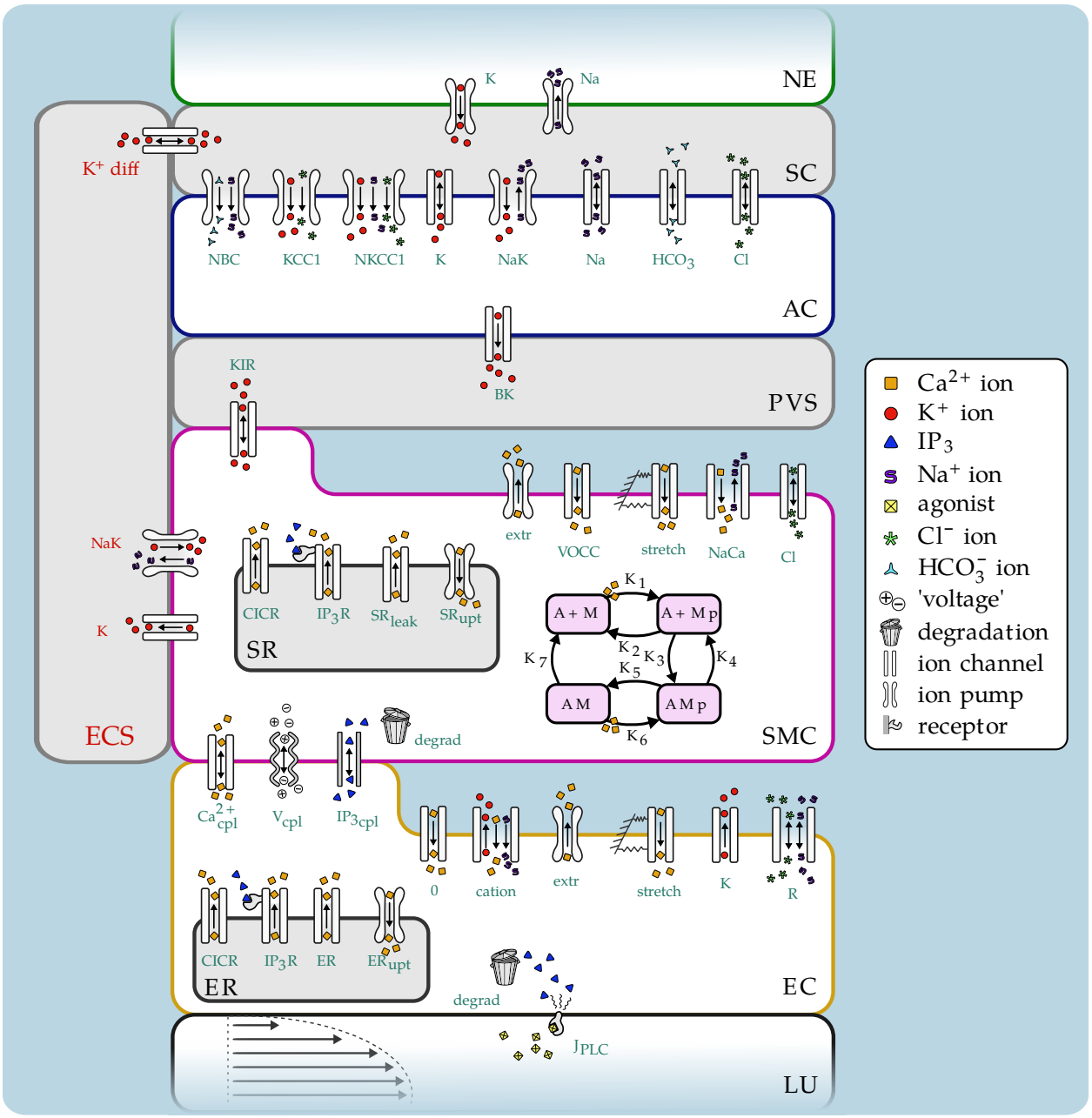

Figure 1: **NVU 1.1.1**. NE: neuron, SC: synaptic cleft, AC: astrocyte, PVS: perivascular space, SMC: smooth muscle cell, SR: sarcoplasmic reticulum, EC: endothelial cell, ER: endoplasmic reticulum, LU: lumen, ECS: extracellular space. K_1 to K_7: wall mechanics reaction rate constants, M: free nonphosphorylated cross bridges, Mp: free phosphorylated cross bridges, AMp: attached phosphorylated cross bridges, AM: attached dephosphorylated latch bridges, KIR: inwardly rectifying potassium channel, BK: large conductance potassium channel, VOCC: voltage operated calcium channel, CICR: calcium induced calcium release channel, IP_3R: IP_3 receptor calcium channel, J_{PLC}: phospholiphase-C dependent IP_3 flux, NaK: sodium potassium pump, K: calcium activated potassium channel. The ECS compartment and fluxes J_{diff}, J_{NaK} and J_K shown in red are new additions to the NVU model.

1.1.1 Extracellular Diffusion in the Tissue Slice (parBrain)

The macro scale simulations incorporate K^+ diffusion between the ECS of adjacent NVU tissue blocks via a linear diffusion term as in Equation (1) with characteristic time τ_e. [**?**] estimated a tissue block size of diameter 400 μm, however arterioles of the cortex perfuse a cylindrical volume of diameter 140 to 320 μm [**?**]. Using the cylindrical diameter value of 140 μm and assuming that the cube shaped tissue blocks each containing a leaf of the H tree (arteriole) perfuse the same volume, the diameter of the tissue blocks is 124 μm. Therefore the characteristic time based on Equation 2 for K^+ to travel through the ECS from one tissue block to another is $\tau_e = 4.3$ sec. All relevant parameters are detailed in Table 1.

Parameter	Value	Unit	Description
τ_s	2.8	s	Characteristic time for diffusion between the SC and ECS
τ_e	4.3	s	Characteristic time for diffusion between adjacent NVU tissue blocks
G_K	4.46e-3	$\mu M m V^{-1} s^{-1}$	Whole SMC conductance for K^+ efflux
w_i	variable	-	Open state probability of calcium activated K^+ channel
v_i	variable	mV	Membrane potential of the SMC
v_K	-94	mV	Nernst potential
F_{NaK}	4.32e-2	$\mu M s^{-1}$	Rate of K^+ influx by the sodium potassium pump

Table 1: Parameters of the NVU model with added ECS compartment.

Diffusion between adjacent NVU tissue blocks is implemented using linear diffusion via the Laplace operator. Diffusion is not implemented for tissue blocks on a diagonal. For a single NVU with coordinates i, j the equation for K_e is given by

$$\frac{dK_e^{i,j}}{dt} = J_K^{i,j} - J_{NaK}^{i,j} - J_{diff}^{i,j} - \frac{1}{\tau_e}\left(4K_e^{i,j} - K_e^{i-1,j} - K_e^{i+1,j} - K_e^{i,j-1} - K_e^{i,j+1}\right). \quad (5)$$

1.1.2 Parallel Implementation

Message Passing Interface (MPI) is used for the communication between tissue blocks in a multi-core architecture, where the MPI communication implements the extracellular diffusion. The simulated tissue slice is split into rectangular domains with each domain corresponding to a single core, whereas the H tree is partitioned into subtrees with a root subtree. For the extracellular diffusion, at each time step the state variables from the blocks along the edges of the domains are passed to the adjacent blocks in the neighbouring domain. Communication between domains and the corresponding boundary conditions enforcement within a single domain is implemented following the mesh ghost block communication pattern [**?**].

2 Code Structure

The three core classes, the `Astrocyte`, `SMCEC` and `WallMechanics`, correspond to the components of the NVU model, namely the astrocyte model, the SMC and EC model, and the mechanical contraction cell model. For a given model component, all fluxes and ODEs are grouped together in the code of the corresponding class. The `NVU` class uses the three core component classes to collect the state variable and derivatives values and pass them to the `ode15s` solver for stiff problems. All classes in OO-NVU code are subclasses of the MATLAB's `handle` class which makes them appear as reference object to avoid unnecessary object duplication on assignment. Figure 2 shows the public interfaces for all OO-NVU classes.

The following features apply to the `Astrocyte`, `SMCEC` and `WallMechanics` classes:

1. The core classes rely on the class constructors to initialise the parameters with the help of the class-specific function parse_inputs(varangin). The constructors also initialise the variable indices, initial conditions and the output indices.

2. In every core class the `rhs` method contains the algebraic and state variables, as well as the corresponding equations.

3. The `shared(self, ~, u)` method, where present, provides the access to the shared algebraic or state variables used as input variables in the other model components where appropriate.

The code in the file `nvu_script.m` provides a number of use-cases for running the NVU model. The code Listing 1 shows an example of setting the options for the ODE solver `ode15s` specifying the `odeopts` parameter, however the code works well with default tolerances. The `simulate()` method of the `NVU` class start the simulation.

Listing 1: Initialisation of the NVU model components.

```
1 odeopts = odeset('RelTol', 1e-03, 'AbsTol', 1e-03, 'MaxStep', 1, ...
      'Vectorized', 1);
2
3 nv = NVU(Astrocyte(), ...
4 WallMechanics(), ...
5 SMCEC('J_PLC', 0.18), ...
6 'odeopts', odeopts);
7
```

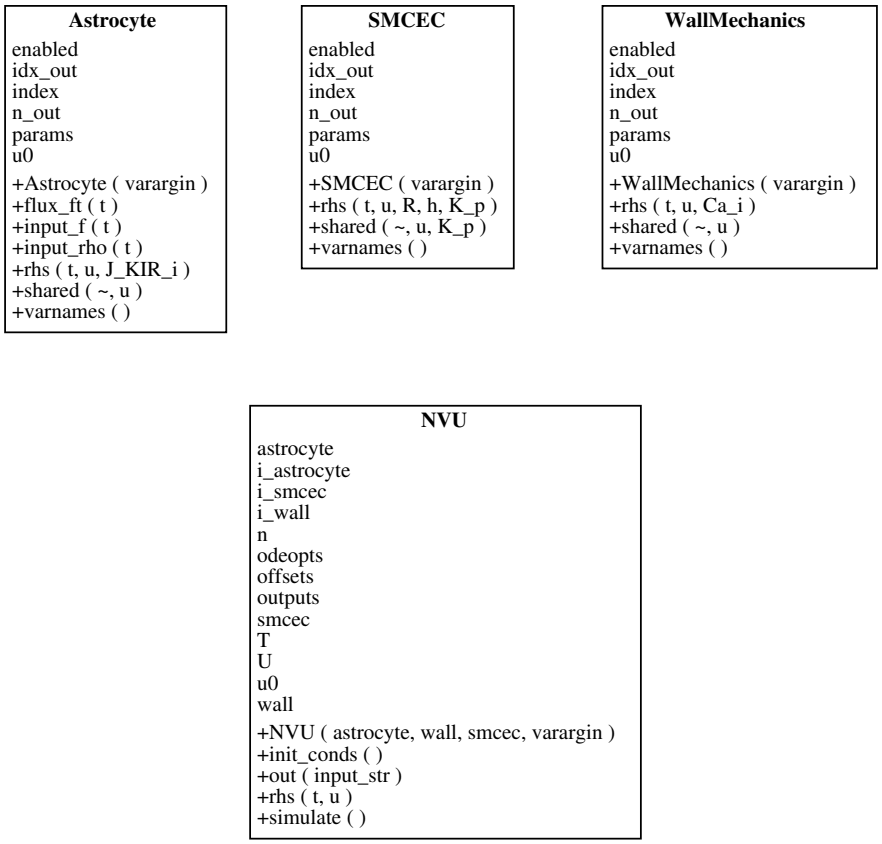

Figure 2: UML class diagram for the OO NVU code.

```
8 nv.simulate()
```

3 Introduction

3.1 Neurovascular Unit

The cerebral cortex, a highly complex component of the human brain and part of the grey matter (*substantia grisea*), mainly consists of neurons (NEs), unmyelinated axons and glial cells such as astrocytes (ACs). It forms the outer layer of *cerebrum* and *cerebellum* and is veined with capillary blood vessels that provide the brain tissue with glucose and oxygen (Shipp [11]). These arterioles are surrounded by endothelial cells (ECs) that form a thin layer on the interior surface of arterioles (*intima*). The outer layer of the arteriole consists of smooth muscle cells (SMCs), which are aligned in circumferential direction. They define the contractile unit of the vessel and regulate its diameter by contraction and dilation.

A neurovascular unit (NVU) defined in this research includes one cell of each of the described types and is graphically pictured in Figure 3.

Each of the cell types and the spaces in between play an important role within the process of neurovascular coupling (NVC, see Section 3.2). The synaptic cleft (SC) is the space between an axon terminal and dendrite of two different NEs in which neurotransmitters are released. It is enclosed by the star-shaped AC that can take up released neurotransmitters. Protoplasmic ACs are polarized cells which can temporarily buffer extracellular K^+, which is one of the key mechanisms within NVC. The astrocytic endoplasmatic reticulum (ER), an isolated space in the cytosol, contains IP_3-sensitive Ca^{2+} channels, which can release Ca^{2+}-ions into the cytosol. The perivascular space (PVS) is located between the end feet of an AC and the arteriole. In the PVS, ion exchange occurs between the arterial wall and the AC. The ECs form a monolayer on the luminal side of the vessel in which all cells are aligned in the direction of the flow. It prevents passive diffusion of bigger molecules, while small ones, such as O_2, Ca^{2+} or IP_3, can pass through. It also functions as an active organ sensing wall shear stress which plays an important role in the NO-mediated pathway. Together with the SMC layer the endothelium forms the blood brain barrier (BBB), the physical frontier between brain tissue and blood vessel. SMC contraction occurs by actin and myosin filaments forming cross-bridges. The rate of contraction is dependent on the SMC cytosolic Ca^{2+} concentration.

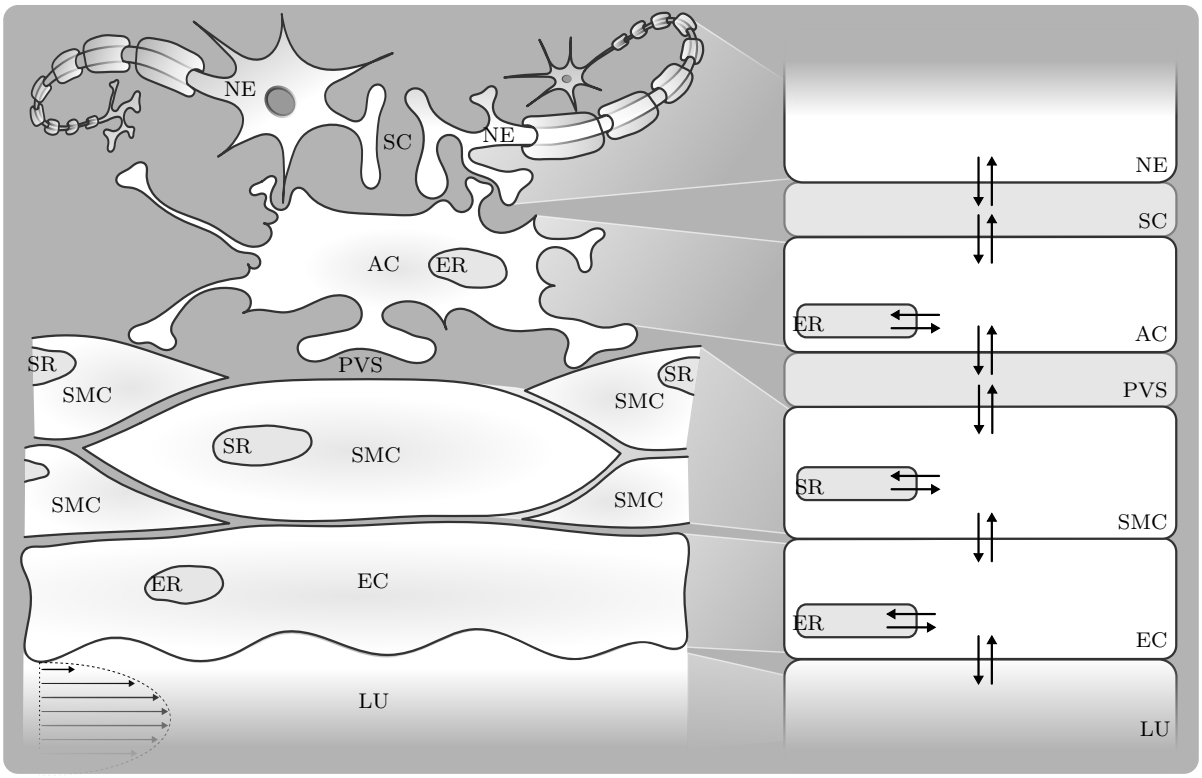

Figure 3: **Overview of different cells and domains that form a neurovascular unit.** NE - Neuron, SC - Synaptic Cleft, AC - Astrocyte, ER - Endoplasmic Reticulum, PVS - Perivascular Space, SMC - Smooth Muscle Cell, SR - Sarcoplasmic Reticulum, EC - Endothelial Cell, LU - Lumen with indicated blood flow. Intercellular communication via the exchange of ions is indicated by arrows.

3.2 Neurovascular Coupling

Neurovascular coupling (NVC), or functional hyperaemia, describes the local vasodilation and -contraction due to neuronal activation. The change in the vessel diameter (vasoreactivity) controls the blood flow and thereby the cerebral supply of oxygen and glucose.

Each cell type plays an important specific role during the process of NVC. Communication between cells is based on an exchange of ions through pumps and channels. These ion fluxes contribute to changes in cytosolic and intercellular species concentration and cell membrane potentials.

There are several pathways that can lead to vasocontraction or -dilation and are mediated by different signalling molecules, such as K^+, Ca^{2+}, EET, NO and 20-HETE. Neurotransmitters are released by the NE into the SC and can bind to receptors on dendrites of other

neurons and astrocytes. This leads to a cascade of chemical reactions and the opening and closing of ion channels which influences the fluxes and concentrations.

3.3 Mathematical Approach

The physiological models are based on a set of differential equations that describe the mass conservation of ions and molecules passing from one cell or domain to another. The simulations describe time-dependent ion fluxes and changes in membrane potential modelled by reaction rates that describe the kinetics which are physiologically validated by experimental data from the literature. This approach assumes homogeneous behaviour of a variable in a certain subdomain i.e. the spatial gradient of a variable in every subdomain is negligible.

4 Existing Models

The present mathematical model is the first of its kind, leading the way in modelling the whole neurovascular coupling process. Starting with the neuronal activation we build up to the response in vessel diameter, utilizing all cell types and crucial pathways. It is based on three existing models.

- **The Astrocyte Model** - describes the crucial biochemical processes within the astrocyte (Ø stby et al. [10], reviewed by Donk and Kock [1]).
- **The SMC and EC Model** - describes the behaviour and the main ion fluxes within the smooth muscle cell (SMC) and endothelium cell (EC). This model is based on that of Koenigsberger et al. [7].
- **The Contraction and Mechanical Model** - describes the relationship between the cytosolic calcium (Ca^{2+}) concentration in the SMC and the contraction and dilation of the SMC by a myosin phosphorylation and cross-bridge based on the models of Hai and Murphy [6] and Kelvin Voigt.

4.1 The Astrocyte Model

During neural activity, K^+ is released into the synaptic cleft (SC) by active neurons (NEs). In the astrocyte model, this is implemented by an influx of K^+ (J_{K_s}) with a corresponding Na^+ uptake by the neuron (J_{Na_s}, Figure **??**). The increase of K^+ in the SC results in an increased K^+ uptake by the AC which consequently undergoes depolarization. This results in a K^+ efflux from distant portions of the cell. Since most of the K^+ conductance of ACs is located at the end-feet, the outward current-carrying K^+ would flow out of the cell largely through these locations. Consequently, the K^+ is 'siphoned' to the end-feet of the astrocyte and released into the perivascular space (PVS) which leads to an increase of K^+ in the PVS. This K^+ release leads to a repolarization of the membrane voltage and is the input signal for the second (SMC & EC) part of this model.

The AC model contains different types of active and passive ion channels. These ion channels and pumps are captured in a set of differential equations to describe the conservation of mass for the corresponding species concentrations in the SC, the AC and the PVS. The ion channels for potassium (J_{KCC1}, J_{NKCC1}, J_K, J_{NaK} and J_{BK}), sodium (J_{NBC}, J_{NKCC1}, J_{NaK} and J_{Na}), chloride (J_{KCC1}, J_{NKCC1} and J_{Cl}) and bicarbonate (J_{HCO_3}) are included.

Note that the bicarbonate and chlorine fluxes are coupled with the Na^+ and K^+ fluxes to obtain a neutral in- or efflux membrane voltage-wise.

4.1.1 Input Signal

In this model, a neuronal excitation was mimicked by an efflux of K^+ into the synaptic cleft (SC) and a simultaneous equal influx of Na^+ into the neuron from the SC (Ø stby et al. [10], see equations in section 5.2). The time-dependent input signal ($f(t)$, see figure 4) starts at $t = 200s$ and ends at $t = 210s$. To estimate the profile $f(t)$ of the K^+ efflux/Na^+ influx, it is assumed that the K^+ efflux has a shape of a beta distribution with the governing parameters α and β such that the profile is optimized according to two criteria [10]:

1. The time from the start until the attaining maximum level of the K^+ concentration in the SC is 5s.
2. The level of the K^+ concentration in the SC at $t = 30$s is 60% of the minimal level.

These two criteria take into account that β is set at a value of $\beta = 5$.

In order to enhance the maximum K^+ level in the SC to reach the order of magnitude proposed by Filosa et al. [2], the amplitude of the input signal $f(t)$ is scaled up by the value F_{input}. The quantity of K^+ ions pumped into the AC can be derived by taking the integral of the flux $k_c f(t)$ over time, where k_c is a constant that relates the input signal $f(t)$ to the K^+ influx.

The amount of released ions are slowly buffered back by the neuron after the input signal terminates. This is modelled by a decay constant within the time interval $230s \leq t \leq 240s$. The integral of this block function is the same as the integral of the beta distribution in order to return to the baseline.

Beside this neuronal input signal, the NKCC1 and KCC1 co-transporters are only enabled when the neuronal ion release and spatial buffering are applied. With both parameters added, the behaviour is modelled by a block function with the value $-F_{input}$ with a default value of zero (Figure 4).

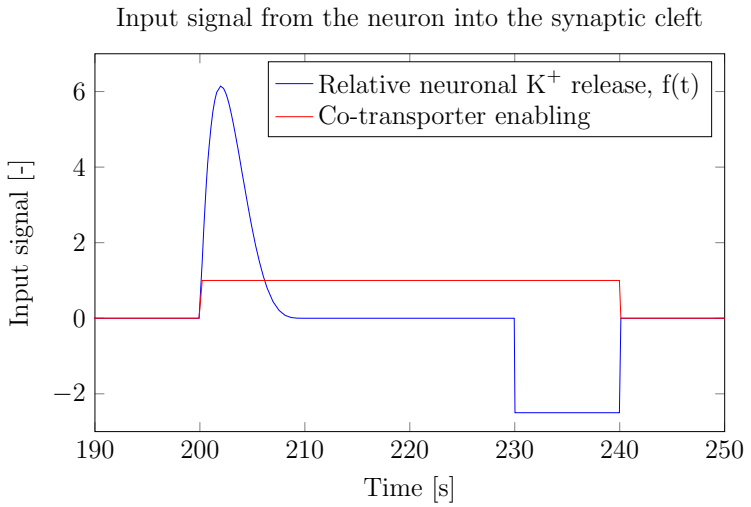

Figure 4: **The input signals used in the astrocyte model.** The K^+ efflux modelled by a beta distribution and buffered back afterwards (blue). The NKCC1 and KCC1 co-transporters are enabled when the neuronal ion release and spatial buffering is applied, modelled by a block function (red).

4.1.2 Scaling

The flux equations used in the AC model are based on the model of Ø stby et al. [10]. Their intention was to look at the volume changes of the AC and SC, therefore the volumes of both are variables in this model and all fluxes are scaled by a volume-surface ratio (R_k and R_s, see Equations 13 and 14, respectively). It is assumed that the sum of the volumes of the AC and SC is a constant (R_{tot}). Due to osmotic pressure, the volume changes. We could show that the changes are comparatively small in our model and it would be justifiable to leave out the scaling factors. However, at the moment they are included because the given fluxes of Ø stby et al. [10] are scaled by the volume-surface ratio. It should be considered in future versions to eliminate the scaling factors by multiplying the fluxes with an adequate constant.

4.2 SMC and EC Model

The SMC and EC model is based on the work of Koenigsberger et al. [7], see Figure 5. This model is extended by adding an inward-rectifier potassium (KIR) channel in the SMC (J_{KIR}, [2]) in order to create a connection between the Astrocyte model and the SMC and EC model.

The input signal for this model is the K^+ concentration in the PVS which is increased by the efflux of astrocytic potassium after neuronal activity.

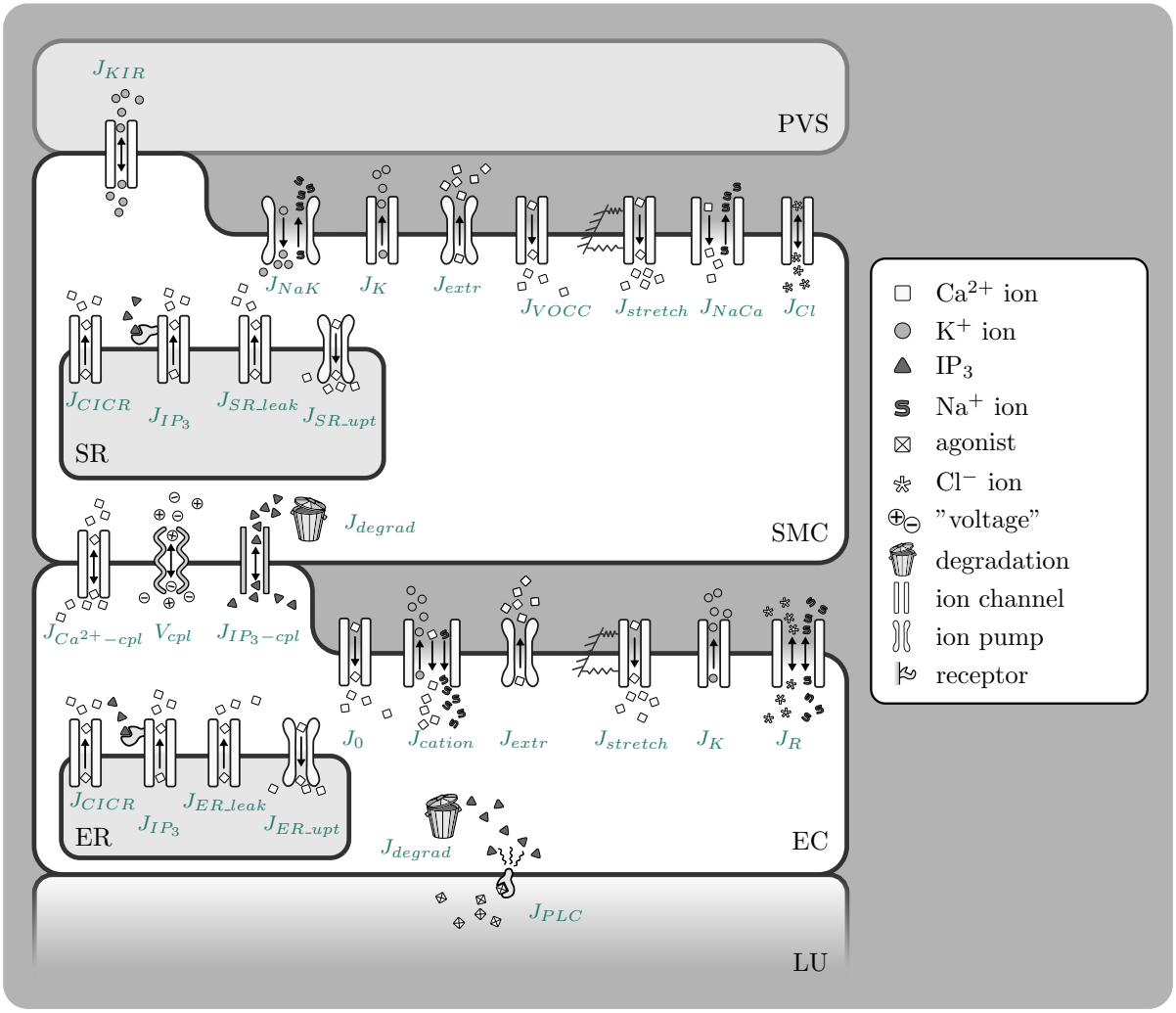

Figure 5: **Illustration of the SMC and EC model.** All modelled fluxes are pictured, note that the indices (k - Astrocyte (AC), s - Synaptic Cleft (SC), p - Perivascular Space (PVS)) are left out for clarity reasons.

The raise in K^+ in the PVS activates the KIR channel on the SMC, causing them to open extruding more potassium into the PVS. This efflux of K^+ hyperpolarizes the SMC membrane and causing the voltage-operated Ca^{2+} channels to close, preventing the influx of Ca^{2+} into the SMC cytosol.

The cytosolic Ca^{2+} concentrations in the SMC and EC and that in the sacroplasmatic

reticulum (SR) and endoplasmatic reticulum (ER), respectively, are described by a set of differential equations. In- and effluxes of K^+ are given by the following ion channel and pumps: J_{KIR}, J_{NaK} and J_K. Ca^{2+} leaves the SR via the channels: J_{CICR}, J_{IP_3} and J_{SR_leak} and enters it by J_{SR_upt}. The in- and efflux of Ca^{2+} are modelled with J_{extr}, J_{VOCC}, $J_{stretch}$ and J_{NaCa}. Note that these fluxes link the cytosol with the extracellular matrix. Here again, a chloride pump is included, J_{Cl}, to return to the resting membrane potential.

Physiologically, ECs and SMCs are connected by gap junctions that allow an intercellular exchange of molecules and voltage. Koenigsberger et al. [7] include the coupling factors $J^{EC-SMC}_{Ca^{2+}-cpl}$, V^{EC-SMC}_{cpl} and $J^{EC-SMC}_{IP_3-cpl}$ for Ca^{2+}, voltage and IP_3 coupling, respectively. The strength of the coupling can be changed in the code with the variable $CASE$.

Inositol triphosphate (IP_3) is an important messenger molecule. It's production, in the endothelium, is triggered by agonist binding onto membrane receptors. IP_3 mediates the J_{IP_3} channel, situated between the reticulum and cytosol. The production rate of IP3 is a constant over time and can be changed by altering the variable J_{PLC} within the mathematical model .

Note that the model of Koenigsberger et al. [7] already includes Ca^{2+}-buffering in the SMC and EC.

4.3 Contraction and Mechanical Model

4.3.1 Contraction Model

The contraction and mechanical part of the model is based on the model of Hai and Murphy [6], which describes the formation of cross bridges between the myosin and actin filaments (Figure 6). This is coupled with a Kelvin-Voigt model that is used to describe the viscoelastic behaviour of the arterial wall (Figure 7).

The Ca^{2+} concentration in the SMC is the input signal for the cross bridge model of Hai and Murphy [6]. The model uses four possible states for the formation of myosin: free nonphosphorylated cross bridges (M), free phosphorylated cross bridges (Mp), attached phosphorylated cross bridges (AMp) and attached dephosphorylated latch bridges (AM). The dynamics of the fraction of myosin in a particular state is given by four differential equations.

The active stress of the SMC is directly proportional to the fraction of attached cross

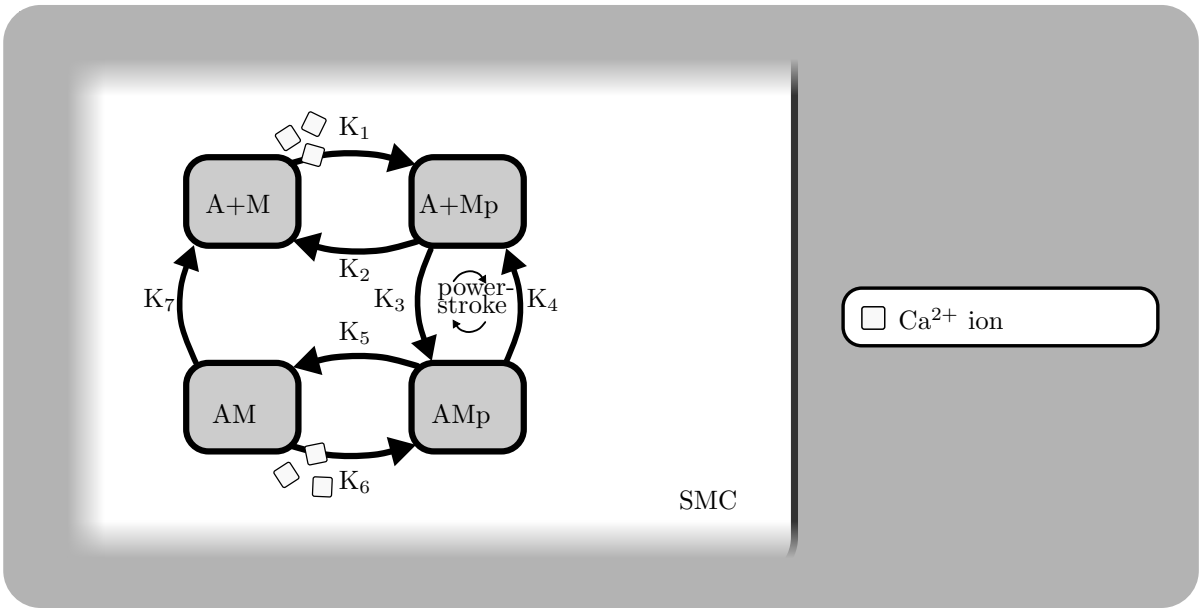

Figure 6: **Illustration of the contraction model within the smooth muscle cell.**

bridges (AM and AMp). Using this model the relation between the cytosolic Ca^{2+} concentration and the active stress of the SMC can be derived.

4.3.2 Mechanical Model

The fraction of attached myosin cross bridges is the input signal for the visco-elastic mechanical model (Kelvin Voigt, Figure 7) which describes the changes in radius over time. The pressure inside the vessel wall is taken as a constant and the circumferential stress is calculated using the Laplacian law.

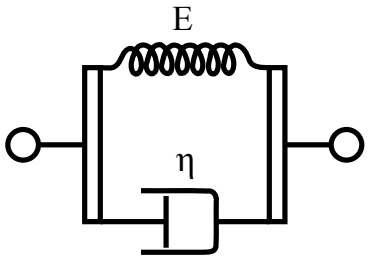

Figure 7: **Schematic overview of a Kelvin Voigt model.**

The Young's modulus and initial radius of the vessel wall is divided into an active and a

passive part and is a function of the attached myosin cross-bridges. The active and passive Young's modulus are based and fitted on experimental data of **?**] which is shown in Figure 8.

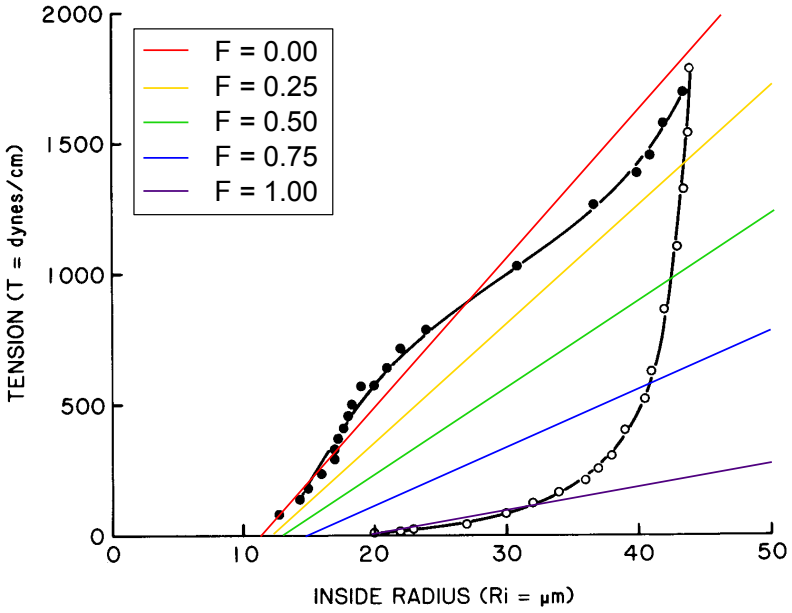

Figure 8: **Linearisation for the Young's modulus and initial radius on the data of ?] for different values of F.**

Figure 8 shows that the initial radius (R_0) decreases when the fraction of attached myosin cross bridges (F) are increased (the intersection with the x-axis). The figure also shows that the Young's modulus, represented by the slope of the lines in the tension-strain graph, increases when F increases. The linearisations of the Young's modulus can be described by:

$$T = \frac{\Delta T}{\Delta R}(R - R_0) \ , \tag{6}$$

where T is the tension of the vessel and $\frac{\Delta T}{\Delta R}$ is the slope of the linearisations in Figure 8.

4.4 Merging of All Models

The Astrocyte model and the SMC and EC model are linked by the SC and the PVS. The K^+ input signal of the neuron is pumped into the SC and taken up afterwards by the AC. The most important ion pumps and channels in this process are the K^+ channels in the neuron which releases the K^+ input, the Na^+/K^+ pump and K^+ channel in the AC which pump the released K^+ into the AC. The result of this is an efflux of K^+ at the end feet of the astrocyte using the BK-channel. Consequently, the membrane voltage of the astrocyte re-polarizes and the K^+ concentration in the PVS increases. This increased K^+ concentration activates the KIR channel in the SMC and start to pump out more K^+ from the SMC into the PVS. The increased efflux of K^+ hyperpolarises the SMC membrane voltage and as a result of that the VOCC closes and prevents the influx of Ca^{2+} into the SMC. Summarising, the neuronal input signal leads to a decrease of Ca^{2+} influx by the VOCC channels and therefore a decrease of the intracellular Ca^{2+} concentration. This leads to a decreased fraction of attached myosin bridges in the Hai and Murphy [6] model, resulting in vessel dilation in the visco-elastic mechanical model.

5 Equations

Some units need to be corrected in this documentation!

5.1 The Extracellular Space Model (new)

Conservation equation of K^+ in the EC (μMs^{-1}):

$$\frac{dK_e}{dt} = J_{K_i} - J_{NaK_i} - J_{diff} \tag{7}$$

Diffusive flux of K^+ from the ECS into the SC (μMs^{-1}):

$$J_{diff} = \frac{1}{\tau_s}\left(K_e - \frac{N_{K_s}}{R_s}\right) \tag{8}$$

J_{K_i}: equation 61. J_{NaK_i}: equation 59.

τ_s	Characteristic diffusion time between the SC and ECS	2.8 s	ME

5.2 The Neuron and Astrocyte Model

Input signals

Neuronal K^+ input signal (dim.less):

$$f_{\mathrm{K/Na}}(t) = \begin{cases} F_{\mathrm{input}} \dfrac{(\alpha_n+\beta_n-1)!}{(\alpha_n-1)!(\beta_n-1)!}\left(\dfrac{1-(t-t_0)}{\Delta t_2}\right)^{\beta_n-1}\left(\dfrac{t-t_0}{\Delta t_2}\right)^{\alpha_n-1}, & \text{for } t_0 \le t < t_1 \\ -F_{\mathrm{input}}, & \text{for } t_2 \le t \le t_3 \\ 0, & \text{otherwise} \end{cases} \tag{9}$$

End of neuronal pulse (s):

$$t_1 = t_0 + \Delta t \tag{10}$$

Start of back-buffering (s):

$$t_2 = t_0 + \Delta t_1 \tag{11}$$

End of back buffering (s):

$$t_3 = t_1 + \Delta t_1 \tag{12}$$

[1]

[1] Model Estimation

F_{input}	amplitude scaling factor	2.67	ME[1]
α_n	beta distribution constant	2	ME
β_n	beta distribution constant	5	ME
t_0	start of neuronal activation	400 s	ME
Δt_1	length of neuronal activation	200 s	ME
Δt_2	time-scaling factor	10 s	[10]

Scaling

AC volume-area ratio (in m):

$$\frac{\mathrm{d}R_k}{\mathrm{d}t} = L_p([\mathrm{Na}^+]_k + [\mathrm{K}^+]_k + [\mathrm{Cl}^-]_k + [\mathrm{HCO}_3^-]_k - [\mathrm{Na}^+]_s - [\mathrm{K}^+]_s - [\mathrm{Cl}^-]_s - [\mathrm{HCO}_3^-]_s + \frac{X_k}{R_k}) \tag{13}$$

SC volume-surface ratio (in m):

$$R_s = R_{\text{tot}} - R_k \tag{14}$$

L_p	total water permeability per unit area of the astrocyte	2.1×10^{-9} m µM^{-1}s^{-1}	[10][2]
X_k	Number of negatively charged impermeable ions trapped within the astrocyte divided by the astrocyte membrane area	12.41×10^{-3} µM m	[10]
R_{tot}	Total volume surface ratio AC + SC ($(V_{sc}+V_k)/A_k$)	8.79×10^{-8} m	[10][2]
A_k	characteristic exchange surface area	3.7×10^{-9} m^2	[10][3]

Conservation Equations

Synaptic Cleft

K^+ concentration in the SC (times the SC volume-area ratio R_s; in µM m):

$$\frac{\mathrm{d}N_{\mathrm{K},s}}{\mathrm{d}t} = k_C f(t) - \frac{\mathrm{d}N_{\mathrm{K},k}}{\mathrm{d}t} - J_{\mathrm{BK},k} \; + R_s J_{diff},; \quad [\mathrm{K}^+]_s = \frac{N_{\mathrm{K},s}}{R_s} \tag{15}$$

Na^+ concentration in the SC (times the SC volume-area ratio R_s; in µM m):

$$\frac{\mathrm{d}N_{\mathrm{Na},s}}{\mathrm{d}t} = -k_C f(t) - \frac{\mathrm{d}N_{\mathrm{Na},k}}{\mathrm{d}t}\,; \quad [\mathrm{Na}^+]_s = \frac{N_{\mathrm{Na},s}}{R_s} \tag{16}$$

[2]corrected value/unit obtained from `CellML`

[3]corrected value/unit obtained from communication with author

HCO_3 concentration in the SC (times the SC volume-area ratio R_s; in µM m):

$$\frac{\mathrm{d}N_{\mathrm{HCO_3},s}}{\mathrm{d}t} = -\frac{\mathrm{d}N_{\mathrm{HCO_3},k}}{\mathrm{d}t}\,; \quad [\mathrm{HCO_3^-}]_s = \frac{N_{\mathrm{HCO_3},s}}{R_s} \tag{17}$$

k_C	Input scaling parameter	7.35×10^{-5} µM m s^{-1}	[10]

Astrocyte

K^+ concentration in the AC (times the AC volume-area ratio R_k; in µM m):

$$\frac{\mathrm{d}N_{\mathrm{K},k}}{\mathrm{d}t} = -J_{\mathrm{K},k} + 2J_{\mathrm{NaK},k} + J_{NKCC1_k} + J_{KCC1_k} - J_{\mathrm{BK},k}\,; \quad [\mathrm{K^+}]_k = \frac{N_{\mathrm{K},k}}{R_k} \tag{18}$$

Na^+ concentration in the AC (times the AC volume-area ratio R_k; in µM m):

$$\frac{\mathrm{d}N_{\mathrm{Na},k}}{\mathrm{d}t} = -J_{\mathrm{Na},k} - 3J_{\mathrm{NaK},k} + J_{NKCC1_k} + J_{\mathrm{NBC},k}\,; \quad [\mathrm{Na^+}]_k = \frac{N_{\mathrm{Na},k}}{R_k} \tag{19}$$

HCO_3 concentration in the AC (times the AC volume-area ratio R_k; in µM m):

$$\frac{\mathrm{d}N_{\mathrm{HCO_3},k}}{\mathrm{d}t} = 2J_{\mathrm{NBC},k}\,; \quad [\mathrm{HCO_3^-}]_k = \frac{N_{\mathrm{HCO_3},k}}{R_k} \tag{20}$$

Cl concentration in the AC (times the AC volume-area ratio R_k; in µM m):

$$\frac{\mathrm{d}N_{\mathrm{Cl},k}}{\mathrm{d}t} = \frac{\mathrm{d}N_{\mathrm{Na},k}}{\mathrm{d}t} + \frac{\mathrm{d}N_{\mathrm{K},k}}{\mathrm{d}t} - \frac{\mathrm{d}N_{\mathrm{HCO_3},k}}{\mathrm{d}t}\,; \quad [\mathrm{Cl^-}]_k = \frac{N_{\mathrm{Cl},k}}{R_k} \tag{21}$$

Open probability of the BK channel (non-dim.):

$$\frac{\mathrm{d}w_k}{\mathrm{d}t} = \phi_w\,(w_\infty - w_k) \tag{22}$$

Perivascular Space

K^+ concentration in the PVS (in µM):

$$\frac{\mathrm{d}K_p}{\mathrm{d}t} = \frac{J_{\mathrm{BK},k}}{R_k R_{pk}} + \frac{J_{\mathrm{KIR},i}}{R_{ps}} - R_{\mathrm{decay}}([\mathrm{K^+}]_p - [\mathrm{K^+}]_{p,\mathrm{min}}); \tag{23}$$

R_{pk}	Volume ratio of PVS to AC	10^{-3} [-]	[9]
R_{ps}	Volume ratio of PVS to SMC	10^{-3} [-]	[9]
R_{decay}	Decay rate	0.05 s^{-1}	M.E.
$[\text{K}^+]_{p,\text{min}}$	min K^+ concentration	3×10^3 µM	M.E.

Fluxes

K^+ flux (times the AC volume-area ratio R_k; in $\mu\text{M}\,\text{m}\,\text{s}^{-1}$):

$$J_{\text{K},k} = \frac{g_{K_k}}{F}(v_k - E_{\text{K},k}) \tag{24}$$

Na^+ flux (times the AC volume-area ratio R_k; in $\mu\text{M}\,\text{m}\,\text{s}^{-1}$):

$$J_{\text{Na},k} = \frac{g_{Na_k}}{F}(v_k - E_{\text{Na},k}) \tag{25}$$

Na^+ and HCO_3 flux through the NBC channel (times the AC volume-area ratio R_k; in $\mu\text{M}\,\text{m}\,\text{s}^{-1}$):

$$J_{\text{NBC},k} = \frac{g_{\text{NBC},k}}{F}\,(v_k - E_{\text{NBC},k}) \tag{26}$$

Cl and K^+ flux through the KCC1 channel (times the AC volume-area ratio R_k; in $\mu\text{M}\,\text{m}\,\text{s}^{-1}$):

$$J_{\text{KCC1},k} = C_{input}\frac{g_{\text{KCC1},k}}{F}\frac{R_{\text{gas}}T}{F} ln\left(\frac{[\text{K}^+]_s[\text{Cl}^-]_s}{K_k[\text{Cl}^-]_k}\right) \tag{27}$$

Na^+, K^+ and Cl flux through the NKCC1 channel (times the AC volume-area ratio R_k; in $\mu\text{M}\,\text{m}\,\text{s}^{-1}$):

$$J_{\text{NKCC1},k} = C_{input}\frac{g_{\text{NKCC1},k}}{F}\frac{R_{\text{gas}}T}{F} ln\left(\frac{Na_s[\text{K}^+]_s{[\text{Cl}^-]_s}^2}{Na_k K_k{[\text{Cl}^-]_k}^2}\right) \tag{28}$$

Flux through the sodium potassium pump (times the AC volume-area ratio R_k; in $\mu\text{M}\,\text{m}\,\text{s}^{-1}$):

$$J_{\text{NaK},k} = J_{\text{NaK,max}}\frac{{Na_k}^{1.5}}{{Na_k}^{1.5} + {K_{\text{Na},k}}^{1.5}}\frac{[\text{K}^+]_s}{[\text{K}^+]_s + K_{\text{K},s}} \tag{29}$$

K^+ flux through the BK channel (times the AC volume-area ratio R_k; in $\mu\text{M}\,\text{m}\,\text{s}^{-1}$):

$$J_{\text{BK},k} = \frac{g_{\text{BK},k}}{F} w_k\,(v_k - E_{\text{BK},k}) \tag{30}$$

Specific ion conductance of the BK channel ($\Omega^{-1}\text{m}^{-2}$):

$$g_{\text{BK},k} = \frac{G_{\text{BK},k} \times 10^{-12}}{A_k} = 1.16 \times 10^3\ \Omega^{-1}\text{m}^{-2} \tag{31}$$

F	Faraday's constant	9.649×10^4 C mol^{-1}	
R_{gas}	Gas constant	8.315 J mol^{-1}K^{-1}	
T	Temperature	300 K	
g_{K_k}	Specific ion conductance of potassium	40×10^3 Ω^{-1}m^{-2}	[10]
$g_{\text{Na},k}$	Specific ion conductance of sodium	1.314×10^3 Ω^{-1}m^{-2}	[10]
$g_{\text{NBC},k}$	Specific ion conductance of the NBC cotransporter	7.57×10^2 Ω^{-1}m^{-2}	[10]
$g_{\text{KCC1},k}$	Specific ion conductance of the KCC1 cotransporter	10 Ω^{-1}m^{-2}	[10]
$g_{\text{NKCC1},k}$	Specific ion conductance of the NKCC1 cotransporter	55.4 Ω^{-1}m^{-2}	[10]
$J_{\text{NaK,max}}$	Maximum flux through the NaKATPase pump	1.42×10^{-3} µM m s^{-1}	[10]
$G_{\text{BK},k}$	Potassium conductance of the BK channel	4.3×10^3 pS	[4]
C_{input}	Block function to switch the channel on and off	0 ; 1 [-]	
$K_{\text{Na},k}$	Michaelis-Menten constant	10^4 µM	
$K_{\text{K},s}$	Michaelis-Menten constant	1.5×10^3 µM	
C_{unit}	Unit converting factor	10^3	M.E.

Additional Equations

Synaptic Cleft

Cl concentration (times the SC volume-area ratio R_s; in µM m):

$$N_{\text{Cl},s} = N_{\text{Na},s} + N_{\text{K},s} - N_{HCO_{3,s}}\,; \quad [\text{Cl}^-]_s = \frac{N_{\text{Cl},s}}{R_s} \tag{32}$$

Astrocyte

Membrane voltage of the AC (V):

$$v_k = \frac{g_{\text{Na},k}E_{\text{Na},k} + g_{\text{K},k}E_{\text{K},k} + g_{\text{Cl},k}E_{\text{Cl},k} + g_{\text{NBC},k}E_{\text{NBC},k} + g_{\text{BK},k}w_kE_{\text{BK},k} - J_{\text{NaK},k}FC_{\text{unit}}}{g_{\text{Na},k} + g_{\text{K},k} + g_{\text{Cl},k} + g_{\text{NBC},k} + g_{\text{BK},k}w_k} \tag{33}$$

Nernst potential for the potassium channel (in mV):

$$E_{\text{K},k} = \frac{R_{\text{gas}}T}{z_KF} ln\left(\frac{[\text{K}^+]_s}{[\text{K}^+]_k}\right) \tag{34}$$

Nernst potential for the sodium channel (in mV):

$$E_{\text{Na},k} = \frac{R_{\text{gas}}T}{z_{\text{Na}}F} ln\left(\frac{Na_s}{Na_k}\right) \tag{35}$$

Nernst potential for the chloride channel (in mV):

$$E_{\text{Cl},k} = \frac{R_{\text{gas}}T}{z_{\text{Cl}}F} ln\left(\frac{[\text{Cl}^-]_s}{[\text{Cl}^-]_k}\right) \tag{36}$$

Nernst potential for the NBC channel (in mV):

$$E_{\mathrm{NBC},k} = \frac{R_{\mathrm{gas}}T}{z_{NBC}F} ln \left(\frac{Na_s {HCO_3}_{,s}^2}{Na_k {HCO_3}_{,k}^2} \right) \tag{37}$$

Nernst potential for the BK channel (in mV):

$$E_{\mathrm{BK},k} = \frac{R_{\mathrm{gas}}T}{z_K F} \ln \left(\frac{[\mathrm{K}^+]_p}{[\mathrm{K}^+]_k} \right) \tag{38}$$

Equilibrium state BK-channel (-):

$$w_\infty = 0.5 \left(1 + \tanh \left(\frac{v_k + v_6}{v_4} \right) \right) \tag{39}$$

Time constant associated with the opening of BK channels (in s^{-1}):

$$\phi_w = \psi_w \cosh \left(\frac{v_k + v_6}{2v_4} \right) \tag{40}$$

$g_{\mathrm{Cl},k}$	Specific ion conductance of chloride	0.879 $\Omega^{-1}\mathrm{m}^{-2}$	[10]
z_K	Valence of a potassium ion	1	
z_{Na}	Valence of a sodium ion	1	
z_{Cl}	Valence of a chloride ion	-1	
z_{NBC}	Effective valence of the NBC cotransporter complex	-1	
v_6	Voltage associated with the opening of half the population	22 mV or V???	[4]
v_4	A measure of the spread of the distribution of the open probability of the BK channel	14.5 mV or V???	[4]
ψ_w	A characteristic time for the open probability of the BK channel	2.664 s^{-1}	[4]

5.3 The Smooth Muscle Cell and Endothelial Cell Model

Conservation Equations

Smooth muscle cell

Cytosolic [Ca^{2+}] in the SMC (in µM):

$$\begin{aligned} \frac{\mathrm{d}[\mathrm{Ca}^{2+}]_i}{\mathrm{d}t} = {} & J_{\mathrm{IP}_3,i} - J_{\mathrm{upt},i} + J_{\mathrm{CICR}_i} - J_{\mathrm{extr},i} + J_{\mathrm{leak},i} \ldots \\ & - J_{\mathrm{VOCC},i} + J_{\mathrm{Na/Ca},i} + 0.1 J_{\mathrm{stretch},i} + J^{SMC-EC}_{Ca^{2+}-coupling_i} \end{aligned} \tag{41}$$

$[Ca^{2+}]$ in the SR of the SMC (in µM):

$$\frac{\mathrm{d}[\widehat{Ca^{2+}}]_i}{\mathrm{d}t} = J_{\mathrm{upt},i} - J_{\mathrm{CICR}_i} - J_{\mathrm{leak},i} \tag{42}$$

Membrane potential of the SMC (in mV):

$$\begin{aligned}\frac{\mathrm{d}v_i}{\mathrm{d}t} = \gamma_i(-J_{\mathrm{Na/K},i} - J_{\mathrm{Cl},i} - 2J_{\mathrm{VOCC},i} - J_{\mathrm{Na/Ca},i} - J_{\mathrm{K},i} \ldots \\ -J_{\mathrm{stretch},i} - J_{\mathrm{KIR},i}) + V^{SMC-EC}_{coupling_i}\end{aligned} \tag{43}$$

Open state probability of calcium-activated potassium channels (dim.less):

$$\frac{\mathrm{d}w_i}{\mathrm{d}t} = \lambda_i \left(K_{act_i} - w_i\right) \tag{44}$$

IP_3 concentration om the SMC (in µM):

$$\frac{\mathrm{d}[\mathrm{IP_3}]_i}{\mathrm{d}t} = J^{SMC-EC}_{IP_3-coupling_i} - J_{\mathrm{degr},i} \tag{45}$$

K^+ concentration in the SMC (in µM):

$$\frac{\mathrm{d}[\mathrm{K^+}]_i}{\mathrm{d}t} = J_{\mathrm{Na/K},i} - J_{\mathrm{KIR},i} - J_{\mathrm{K},i} \tag{46}$$

γ_i	Change in membrane potential by a scaling factor	1970 $\mathrm{mV\mu M^{-1}}$	[7]
λ_i	Rate constant for opening	45.0 s^{-1}	[7]

Endothelial cell

Cytosolic Ca^{2+} concentration in the EC (in µM):

$$\begin{aligned}\frac{\mathrm{d}[\mathrm{Ca^{2+}}]_j}{\mathrm{d}t} = J_{\mathrm{IP_3},j} - J_{\mathrm{upt},j} + J_{CICR_j} - J_{\mathrm{extr},j} \ldots \\ +J_{\mathrm{leak},j} + J_{cation_j} + J_{0_j} + J_{\mathrm{stretch},j} - J^{SMC-EC}_{Ca^{2+}-coupling_j}\end{aligned} \tag{47}$$

Ca^{2+} concentration in the ER in the EC (in µM):

$$\frac{\mathrm{d}[\widehat{\mathrm{Ca^{2+}}}]_j}{\mathrm{d}t} = J_{\mathrm{upt},j} - J_{CICR_j} - J_{\mathrm{leak},j} \tag{48}$$

Membrane potential of the EC (in mV):

$$\frac{\mathrm{d}v_j}{\mathrm{d}t} = -\frac{1}{C_{m_j}}(J_{K_j} + J_{R_j}) + V^{SMC-EC}_{coupling_j} \tag{49}$$

IP_3 concentration of the EC (in µM):

$$\frac{\mathrm{d}[\mathrm{IP_3}]_j}{\mathrm{d}t} = J_{\mathrm{EC,IP_3}} - J_{\mathrm{degr},j} - J^{SMC-EC}_{IP_3-coupling_j} \tag{50}$$

C_{m_j}	Membrane capacitance	25.8 pF	[7]
J_{PLC}	PLC / IP_3 production rate	0.18 or 0.4 $\mu M\,s^{-1}$	[7]
J_{0_j}	Constant Ca2+ leak term (influx)	0.029 $\mu M\,s^{-1}$	[7]

Fluxes

Smooth muscle cell

Release of calcium from IP_3 sensitive stores in the SMC (in $\mu M\,s^{-1}$):

$$J_{\mathrm{IP_3},i} = F_i \frac{[\mathrm{IP_3}]_i^2}{K_{ri}^2 + [\mathrm{IP_3}]_i^2} \tag{51}$$

F_i	Maximal rate of activation-dependent calcium influx	0.23 $\mu M\,s^{-1}$	[7]
K_{ri}	Half-saturation constant for agonist-dependent calcium entry	1 µM	[7]

Uptake of calcium into the sarcoplasmic reticulum (in $\mu M\ s^{-1}$):

$$J_{\mathrm{upt},i} = B_i \frac{{[\mathrm{Ca^{2+}}]_i}^2}{c_{bi}^2 + {[\mathrm{Ca^{2+}}]_i}^2} \tag{52}$$

B_i	SR uptake rate constant	2.025 $\mu M\ s^{-1}$	[7]
c_{bi}	Half-point of the SR ATPase activation sigmoidal	1.0 µM	[7]

Calcium-induced calcium release (CICR; in $\mu M\ s^{-1}$):

$$J_{\mathrm{CICR}_i} = C_i \frac{{[\widehat{\mathrm{Ca^{2+}}}]_i}^2}{s_{ci}^2 + {[\widehat{\mathrm{Ca^{2+}}}]_i}^2} \frac{{[\mathrm{Ca^{2+}}]_i}^4}{c_{ci}^4 + {[\mathrm{Ca^{2+}}]_i}^4} \tag{53}$$

C_i	CICR rate constant	55 $\mu M\ s^{-1}$	[7]
s_{ci}	Half-point of the CICR Ca^{2+} efflux sigmoidal	2.0 µM	[7]
c_{ci}	Half-point of the CICR activation sigmoidal	0.9 µM	[7]

Calcium extrusion by Ca^{2+}-ATPase pumps (in $\mu M\ s^{-1}$):

$$J_{\mathrm{extr},i} = D_i [\mathrm{Ca^{2+}}]_i \left(1 + \frac{v_i - v_d}{R_{di}}\right) \tag{54}$$

D_i	Rate constant for Ca^{2+} extrusion by the ATPase pump	0.24 s^{-1}	[7]
v_d	Intercept of voltage dependence of extrusion ATPase	-100.0 mV	[7]
R_{di}	Slope of voltage dependence of extrusion ATPase.	250.0 mV	[7]

Leak current from the SR (in µM s^{-1}):

$$J_{\text{leak},i} = L_i[\widehat{\text{Ca}^{2+}}]_i \tag{55}$$

L_i	Leak from SR rate constant	0.025 s^{-1}	[7]

Calcium influx through VOCCs (in µM s^{-1}):

$$J_{\text{VOCC},i} = G_{\text{Ca},i}\frac{v_i - v_{\text{Ca}_1,i}}{1 + \exp(-\left[\left(v_i - v_{\text{Ca}_2,i}\right)/R_{\text{Ca},i}\right])} \tag{56}$$

$G_{\text{Ca},i}$	Whole-cell conductance for VOCCs	1.29×10^{-3} µM $mV^{-1}s^{-1}$	[7]
$v_{\text{Ca}_1,i}$	Reversal potential for VOCCs	100.0 mV	[7]
$v_{\text{Ca}_2,i}$	Half-point of the VOCC activation sigmoidal	-24.0 mV	[7]
$R_{\text{Ca},i}$	Maximum slope of the VOCC activation sigmoidal	8.5 mV	[7]

Flux of calcium exchanging with sodium in the Na^+Ca^{2+} exchange (in µM s^{-1}):

$$J_{\mathrm{Na/Ca},i} = G_{\mathrm{Na/Ca},i} \frac{[\mathrm{Ca}^{2+}]_i}{[\mathrm{Ca}^{2+}]_i + c_{\mathrm{Na/Ca},i}} \left(v_i - v_{\mathrm{Na/Ca},i}\right) \tag{57}$$

$G_{\mathrm{Na/Ca},i}$	Whole-cell conductance for Na^+/Ca^{2+} exchange	3.16×10^{-3} µM $mV^{-1}s^{-1}$	[7]
$c_{\mathrm{Na/Ca},i}$	Half-point for activation of Na^+/Ca^{2+} exchange by Ca^{2+}	0.5 µM	[7]
$v_{\mathrm{Na/Ca},i}$	Reversal potential for the Na^+/Ca^{2+} exchanger	-30.0 mV	[7]

Calcium flux through the stretch-activated channels in the SMC (in µM s^{-1}):

$$J_{\mathrm{stretch},i} = \frac{G_{\mathrm{stretch}}}{1 + \exp\left(-\alpha_{\mathrm{stretch}}\left(\frac{\Delta p R}{h} - \sigma_0\right)\right)} \left(v_i - E_{\mathrm{SAC}}\right) \tag{58}$$

G_{stretch}	Whole cell conductance for SACs	6.1×10^{-3} µM $mV^{-1}s^{-1}$	[7]
$\alpha_{\mathrm{stretch}}$	Slope of stress dependence of the SAC activation sigmoidal	7.4×10^{-3} $mmHg^{-1}$	[7]
Δp	Pressure difference	30 mmHg	ME
σ_0	Half-point of the SAC activation sigmoidal	500 mmHg	[7]
E_{SAC}	Reversal potential for SACs	-18 mV	[7]

Flux through the sodium potassium pump (in µM s^{-1}):

$$J_{\mathrm{Na/K},i} = F_{\mathrm{Na/K},i} \tag{59}$$

$F_{\mathrm{Na/K},i}$	Rate of the potassium influx by the sodium potassium pump	4.32×10^{-2} µM s^{-1}	[7]

Chloride flux through the chloride channel (in µM s^{-1}):

$$J_{\mathrm{Cl},i} = G_{\mathrm{Cl},i}\left(v_i - v_{\mathrm{Cl},i}\right) \tag{60}$$

Potassium flux through potassium channel (in µM s^{-1}):

$$J_{\mathrm{K},i} = G_{\mathrm{K},i} w_i \left(v_i - v_{K_i}\right) \tag{61}$$

$G_{\mathrm{Cl},i}$	Whole-cell conductance for Cl^- current	1.34×10^{-3} µM $mV^{-1}s^{-1}$	[7]
$v_{\mathrm{Cl},i}$	Reversal potential for Cl^- channels.	-25.0 mV	[7]

$G_{\mathrm{K},i}$	Whole-cell conductance for K^+ efflux.	4.46×10^{-3} µM $mV^{-1}s^{-1}$	[7]
v_{K_i}	Nernst potential	-94 mV	[7]

Flux through KIR channels in the SMC (in µM s^{-1}):

$$J_{\mathrm{KIR},i} = \frac{F_{\mathrm{KIR},i} g_{\mathrm{KIR},i}}{\gamma_i}(v_i - v_{\mathrm{KIR},i}) \tag{62}$$

$F_{\mathrm{KIR},i}$	Scaling factor of potassium efflux through the KIR channel	750 mV μM^{-1}	[4]

IP_3 degradation (in µM s^{-1}):

$$J_{\mathrm{degr},i} = k_{\mathrm{d},i}[\mathrm{IP_3}]_i \tag{63}$$

$k_{\mathrm{d},i}$	Rate constant of IP_3 degradation	0.1 s^{-1}	[7]

Endothelial cell

Release of calcium from IP_3-sensitive stores in the EC (in µM s^{-1}):

$$J_{\mathrm{IP_3},j} = F_j \frac{[\mathrm{IP_3}]_j^2}{K_{rj}^2 + [\mathrm{IP_3}]_j^2} \tag{64}$$

F_j	Maximal rate of activation-dependent calcium influx	0.23 µM s^{-1}	[7]
K_{rj}	Half-saturation constant for agonist-dependent calcium entry	1 µM	[7]

Uptake of calcium into the endoplasmic reticulum (in µM s^{-1}):

$$J_{\mathrm{upt},j} = B_j \frac{{[\mathrm{Ca^{2+}}]_j}^2}{c_{bj}^2 + {[\mathrm{Ca^{2+}}]_j}^2} \tag{65}$$

B_j	ER uptake rate constant	0.5 µM s^{-1}	[7]
c_{bj}	Half-point of the SR ATPase activation sigmoidal	1.0 µM	[7]

Calcium-induced calcium release (CICR; in µM s^{-1}):

$$J_{CICR_j} = C_j \frac{\left[\widehat{\mathrm{Ca}^{2+}}\right]_j^{\,2}}{s_{cj}^2 + \left[\widehat{\mathrm{Ca}^{2+}}\right]_j^{\,2}} \frac{\left[\mathrm{Ca}^{2+}\right]_j^{\,4}}{c_{cj}^4 + \left[\mathrm{Ca}^{2+}\right]_j^{\,4}} \tag{66}$$

C_j	CICR rate constant	5 µM s^{-1}	[7]
s_{cj}	Half-point of the CICR Ca^{2+} efflux sigmoidal	2.0 µM	[7]
c_{cj}	Half-point of the CICR activation sigmoidal	0.9 µM	[7]

Calcium extrusion by Ca^{2+}-ATPase pumps (in µM s^{-1}):

$$J_{\mathrm{extr},j} = D_j[\mathrm{Ca}^{2+}]_j \tag{67}$$

D_j	Rate constant for Ca^{2+} extrusion by the ATPase pump	0.24 s^{-1}	[8]

Calcium flux through the stretch-activated channels in the EC (in µM s^{-1}):

$$J_{\mathrm{stretch},j} = \frac{G_{\mathrm{stretch}}}{1 + e^{-\alpha_{\mathrm{stretch}}(\sigma - \sigma_0)}} (v_j - E_{\mathrm{SAC}}) = \frac{G_{\mathrm{stretch}}}{1 + e^{-\alpha_{\mathrm{stretch}}\left(\frac{\Delta p R}{h} - \sigma_0\right)}} (v_j - E_{\mathrm{SAC}}) \tag{68}$$

G_{stretch}	The whole cell conductance for SACs	6.1×10^{-3} µM $mV^{-1}s^{-1}$	[7]
$\alpha_{\mathrm{stretch}}$	Slope of stress dependence of the SAC activation sigmoidal	7.4×10^{-3} $mmHg^{-1}$	[7]
Δp	Pressure difference	30 mmHg	ME
σ_0	Half-point of the SAC activation sigmoidal	500 mmHg	[7]
E_{SAC}	The reversal potential for SACs	-18 mV	[7]

table ist dop-pelt?!

Leak current from the ER (in µM s^{-1}):

$$J_{\mathrm{leak},j} = L_j[\widehat{\mathrm{Ca}^{2+}}]_j \tag{69}$$

L_j	Rate constant for Ca^{2+} leak from the ER	0.025 s^{-1}	[7]

Calcium influx through nonselective cation channels (in µM s^{-1}):

$$J_{cation_j} = G_{cat_j}(E_{Ca_j} - v_j)\frac{1}{2}\left(1 + \tanh\left(\frac{\log_{10}[Ca^{2+}]_j - m_{3_{cat_j}}}{m_{4_{cat_j}}}\right)\right) \tag{70}$$

G_{catj}	Whole-cell cation channel conductivity	6.6×10^{-4} µM $mV^{-1}s^{-1}$	[7]
E_{Caj}	Ca^{2+} equilibrium potential	50 mV	[7]
$m_{3_{catj}}$	Model constant	-0.18 µM	[7]
$m_{4_{catj}}$	Model constant	0.37 µM	[7]

Potassium efflux through the $J_{BK_{Caj}}$ channel and the $J_{SK_{Caj}}$ channel (in µM s^{-1}):

$$J_{K_j} = G_{totj}(v_j - v_{Kj})\left(J_{BK_{Caj}} + J_{SK_{Caj}}\right) \tag{71}$$

G_{totj}	Total potassium channel conductivity.	6927 pS	[7]
v_{Kj}	K^+ equilibrium potential	-80.0 mV	[7]

Potassium efflux through the $J_{BK_{Caj}}$ channel (in µM s^{-1}):

$$J_{BK_{Caj}} = 0.2\left(1 + \tanh\left(\frac{(\log_{10}[Ca^{2+}]_j - c)(v_j - b_j) - a_{1j}}{m_{3bj}(v_j + a_{2j}(\log_{10}[Ca^{2+}]_j - c) - b_j)^2 + m_{4bj}}\right)\right) \tag{72}$$

Potassium efflux through the $J_{SK_{Caj}}$ channel (in µM s^{-1}):

$$J_{SK_{Caj}} = 0.3\left(1 + \tanh\left(\frac{\log_{10}[Ca^{2+}]_j - m_{3sj}}{m_{4sj}}\right)\right) \tag{73}$$

Residual current regrouping chloride and sodium current flux (in µM s^{-1}):

$$J_{R_j} = G_{R_j}(v_j - v_{\text{rest},j}) \tag{74}$$

IP_3 degradation (in µM s^{-1}):

$$J_{\text{degr},j} = k_{\text{d},j}[IP_3]_j \tag{75}$$

c	Model constant, further explanation see reference	-0.4 µM	[7]
b_j	Model constant, further explanation see reference	-80.8 mV	[7]
a_{1j}	Model constant, further explanation see reference	53.3 µM mV	[7]
a_{2j}	Model constant, further explanation see reference	53.3 mVµM^{-1}	[7]
m_{3bj}	Model constant, further explanation see reference	1.32×10^{-3} µM mV^{-1}	[7]
m_{4bj}	Model constant, further explanation see reference	0.30 µM mV	[7]
m_{3sj}	Model constant, further explanation see reference	-0.28 µM	[7]
m_{4sj}	Model constant, further explanation see reference	0.389 µM	[7]
G_{R_j}	Residual current conductivity	955 pS	[7]
$v_{\text{rest},j}$	Membrane resting potential	-31.1 mV	[7]
$k_{\text{d},j}$	Rate constant of IP_3 degradation	0.1 s^{-1}	[7]

Coupling

Heterocellular electrical coupling between SMCs and ECs (in mV s^{-1}):

$$V_{coupling_i}^{SMC-EC} = -G_{coup}(v_i - v_j) \tag{76}$$

Heterocellular IP_3 coupling between SMCs and ECs (in µM s^{-1}):

$$J_{IP_3-coupling_i}^{SMC-EC} = -P_{IP_3}([\mathrm{IP_3}]_i - [\mathrm{IP_3}]_j) \tag{77}$$

Calcium coupling with EC (in µM s^{-1}):

$$J_{Ca^{2+}-coupling_i}^{SMC-EC} = -P_{Ca^{2+}}([\mathrm{Ca^{2+}}]_i - [\mathrm{Ca^{2+}}]_j) \tag{78}$$

G_{coup}	Heterocellular electrical coupling coefficient	0.5 s^{-1}	ME
P_{IP_3}	Heterocellular IP_3 coupling coefficient	0.05 s^{-1}	[7]
$P_{Ca^{2+}}$	Heterocellular $P_{Ca^{2+}}$ coupling coefficient	0.05 s^{-1}	[7]

Additional Equations

Equilibrium distribution of open channel states for the voltage and calcium activated potassium channels (dimensionless):

$$K_{act_i} = \frac{([\mathrm{Ca^{2+}}]_i + c_{wi})^2}{([\mathrm{Ca^{2+}}]_i + c_{wi})^2 + \beta_i \exp(-([v_i - v_{Ca_{3i}}]/R_{Ki}))} \tag{79}$$

Nernst potential of the KIR channel in the SMC (in mV):

$$v_{\mathrm{KIR},i} = z_1[\mathrm{K}^+]_p - z_2 \tag{80}$$

Conductance of KIR channel (in µM mV^{-1} s^{-1}):

$$g_{\mathrm{KIR},i} = \exp(z_5 v_i + z_3[\mathrm{K}^+]_p - z_4) \tag{81}$$

c_{wi}	Translation factor for Ca^{2+} dependence of K_{Ca} channel activation sigmoidal.	0.0 µM	[7]
β_i	Translation factor for membrane potential dependence of K_{Ca} channel activation sigmoidal.	0.13 μM^2	[7]
$v_{Ca_{3i}}$	Half-point for the K_{Ca} channel activation sigmoidal.	-27 mV	[7]
R_{Ki}	Maximum slope of the K_{Ca} activation sigmoidal.	12 mV	[7]
z_1	Model estimation for membrane voltage KIR channel	4.5×10^3 $\mathrm{mV\mu M^{-1}}$	[3]
z_2	Model estimation for membrane voltage KIR channel	112 mV	[3]
z_3	Model estimation for the KIR channel conductance	4.2×10^2 $\mathrm{mV^{-1}s^{-1}}$	[3]
z_4	Model estimation for the KIR channel conductance	12.6 µM $\mathrm{mV^{-1}s^{-1}}$	[3]
z_5	Model estimation for the KIR channel conductance	-7.4×10^{-2} µM $\mathrm{mV^{-2}s^{-1}}$	[3]

5.4 The Contraction Model

Fraction of free phosphorylated cross-bridges (dimensionless):

$$\frac{\mathrm{d}[Mp]}{\mathrm{d}t} = K_4[AMp] + K_1[M] - (K_2 + K_3)[Mp] \tag{82}$$

Fraction of attached phosphorylated cross-bridges (dimensionless):

$$\frac{\mathrm{d}[AMp]}{\mathrm{d}t} = K_3[Mp] + K_6[AM] - (K_4 + K_5)[AMp] \tag{83}$$

Fraction of attached dephosphorylated cross-bridges (dimensionless):

$$\frac{\mathrm{d}[AM]}{\mathrm{d}t} = K_5[AMp] - (K_7 + K_6)[AM] \tag{84}$$

Fraction of free non-phosphorylated cross-bridges (dimensionless):

$$[M] = 1 - [AM] - [AMp] - [Mp] \tag{85}$$

Rate constants that represent phosphorylation of M to Mp and of AM to AMp by the active myosin light chain kinase (MLCK), respectively (in s^{-1}):

$$K_1 = K_6 = \gamma_{cross}[\mathrm{Ca}^{2+}]_i^{\,n_{cross}} \tag{86}$$

K_2	Rate constant for dephosphorylation (of Mp to M) by myosin light-chain phosphatase (MLCP)	0.5 s^{-1}	[6]
K_3	Rate constants representing the attachment/detachment of fast cycling phosphorylated crossbridges	0.4 s^{-1}	[6]
K_4	Rate constants representing the attachment/detachment of fast cycling phosphorylated crossbridges	0.1 s^{-1}	[6]
K_5	Rate constant for dephosphorylation (of AMp to AM) by myosin light-chain phosphatase (MLCP)	0.5 s^{-1}	[6]
K_7	Rate constant for latch-bridge detachment	0.1 s^{-1}	[6]
γ_{cross}	Sensitivity of the contractile apparatus to calcium	17 μM^{-3} s^{-1}	[8]
n_{cross}	Fraction constant of the phosphorylation crossbridge	3 [–]	[8]

5.5 The Mechanical Model

Wall thickness of the vessel (in µm):

$$h = 0.1R \tag{87}$$

Fraction of attached myosin cross-bridges (dimensionless):

$$F_r = [AM_p] + [AM] \tag{88}$$

Vessel radius (in m):

$$\frac{\mathrm{d}R}{\mathrm{d}t} = \frac{R_{0_{pas}}}{\eta}\left(\frac{RP_T}{h} - E(F_r)\frac{R - R_0(F_r)}{R_0(F_r)}\right) \tag{89}$$

with:

$$E(F_r) = E_{pas} + F_r\left(E_{act} - E_{pas}\right) \tag{90}$$

$$R_0(F_r) = R_{0_{pas}} + F_r(\alpha_r - 1)R_{0_{pas}} \tag{91}$$

η	viscosity	10^4 Pa s	[7]
$R_{0_{pas}}$	Radius of the vessel when passive and no stress is applied	20 µm	ME
P_T	Transmural pressure	4×10^3 Pa	ME
E_{pas}	Young's modulus for the passive vessel	66×10^3 Pa	[5]
E_{act}	Young's modulus for the active vessel	233×10^3 Pa	[5]
α_r	Scaling factor initial radius	0.6	[5]

References

[1] **Donk, L. V. D. and Kock, E. G. J. D.** (**2013**): Bluefern Supercomputing Unit University of Canterbury Eindhoven University of Technology.

[2] **Filosa, J. A.; Bonev, A. D. and Nelson, M. T.** (**2004**): Calcium dynamics in cortical astrocytes and arterioles during neurovascular coupling., Circulation research, Vol. 95, No. 10 pp. e73–81.

[3] **Filosa, J. a.; Bonev, A. D.; Straub, S. V.; Meredith, A. L.; Wilkerson, M. K.; Aldrich, R. W. and Nelson, M. T.** (**2006**): Local potassium signaling couples neuronal activity to vasodilation in the brain., Nature neuroscience, Vol. 9, No. 11 pp. 1397–1403.

[4] **Gonzalez-fernandez, J. M. and Ermentrout, B.** (**1994**): On the origin and dynamics of the vasomotion of small arteries, Mathematical biosciences, Vol. 119, No. 2 pp. 127–167.

[5] **Gore, R. W. and Davis, M. J.** (**1985**): Mechanics of Smooth Muscle in Isolated Single Microvessels, Vol. 12 pp. 511–520.

[6] **Hai, C.-m. and Murphy, R. A.** (**1989**): Ca2+ Crossbridge Phosphorylation, and Contraction, Annual review of physiology, Vol. 51, No. 1 pp. 285–298.

[7] **Koenigsberger, M.; Sauser, R.; Bény, J.-L. J. and Meister, J. J.-J.** (**2006**): Effects of arterial wall stress on vasomotion, Biophysical journal, Vol. 91, No. September pp. 1663–1674.

[8] **Koenigsberger, M.; Sauser, R.; Bény, J.-L. L.; Meister, J.-J. J. and Be, J.-l.** (**2005**): Role of the endothelium on arterial vasomotion, Biophysical journal, Vol. 88, No. 6 pp. 3845–3854.

[9] **Nagelhus, E.; Horio, Y. and Inanobe, A.** (**1999**): Immunogold evidence suggests that coupling of K+ siphoning and water transport in rat retinal muller cells is mediated by a coenrichment of kir4. 1 and aqp4 in specific membrane domains, Glia, Vol. 63, No. 1 pp. 47–54.

[10] **Ø stby, I.; Ø yehaug, L.; Einevoll, G. T.; Nagelhus, E. A.; Plahte, E.; Zeuthen, T.; Lloyd, C. M.; Ottersen, O. P. and Omholt, S. W.** (**2009**): Astrocytic Mechanisms Explaining Neural-Activity-Induced Shrinkage of Extraneuronal Space, PLoS Computational Biology, Vol. 5, No. 1 pp. 1–12.

[11] **Shipp, S.** (**2007**): Structure and function of the cerebral cortex., Current biology : CB, Vol. 17, No. 12 pp. R443—-9.

[12] **Syková, E. and Nicholson, C.** (**2008**): Diffusion in brain extracellular space., Physiological reviews, Vol. 88, No. 4 pp. 1277–1340.

[13] **Witthoft, A. and Em Karniadakis, G.** (**2012**): A bidirectional model for communication in the neurovascular unit., Journal of theoretical biology, Vol. 311 pp. 80–93.